Reverse-Flow Centrifugal Separators in Parallel: Performance and Flow Pattern

Weiming Peng and Alex C. Hoffmann
Department of Physics and Technology, University of Bergen, Allegt 55, 5007 Bergen, Norway

Huub Dries, Michiel Regelink, and Kee-Khoon Foo
Shell Global Solutions, Shell Amsterdam, PO Box 38000, 1030 BN Amsterdam, The Netherlands

DOI 10.1002/aic.11121
Published online February 2, 2007 in Wiley InterScience (www.interscience.wiley.com).

The results obtained by performance tests and flow visualization in a model swirl deck, containing 8 reverse-flow swirl tubes working in parallel being charged from and discharging to common plenums. Various features specific to such arrangements, such as the phenomenon of cross-talk, where flow from one tube to the other takes place in the dust collection plenum, are discussed in light of the results. The performance of the deck is compared to that of a single geometrically similar tube by Stokesian scaling. This comparison shows that the performance of this deck is not seriously reduced by effects such as cross-talk. The appearance of dancing rings in the tubes reveal the presence of the end of the vortex in the tubes, a fact that impacts the phenomenon of cross-talk. The end of the vortex was further studied using high-time-resolution pressure sensors. The flowpattern in the dust plenum was studied using neutral density tracers with normal and high-speed photography. The impact of various modifications to the deck, such as artificially roughening a tube, reducing the volume of the dust plenum to exacerbate cross-talk, and lengthening the individual tubes to improve separation performance are discussed. © 2007 American Institute of Chemical Engineers *AIChE J,* 53: 589–597, 2007

Keywords: cyclone separators, swirl tubes in parallel, separation efficiency, gas purification, aerosols

Introduction

In a reverse flow swirl tube separator, the gas swirls downward in the outer part of the separation space, the particles being centrifuged out to the wall. The gas reverses its axial flow direction as it moves inward and spins upward in the central part, exiting through the vortex finder. The particles leave the swirl tube through the bottom, which may or may not be equipped with a base plate leaving an annular gap through which the particles flow.

Swirl tubes are often used in final-stage, high-efficiency dedusters operating at moderate or low-solids loadings. The tubes are mostly arranged in parallel with a large number of smaller tubes in "swirl deck" or "multicyclone", in which they are fed from—and discharge to—common plenums. An example of such an arrangement, namely the swirl deck model used for this work, is shown in Figure 1.

A well-known problem phenomenon in such arrangements is that of "cross-talk".[1] It occurs when the flow is maldistributed between the cyclones and the cyclone underflows—as in this case—are not isolated (sealed) from one another. A nonuniform flow to the cyclones produces a variation in pressure within the solids discharge piping of the individual cyclones giving rise to flow between the tubes in the dust plenum. When cross-talk occurs, one speaks of "donor" tubes that have more gas passing through the vanes than exiting the vortex tube (donates gas to the hopper), and "receptor" tubes, where more gas leaves the vortex tube than enters through the vanes (pulls

Correspondence concerning this article should be addressed to A. C. Hoffmann at alex.hoffmann@ift.uib.No.
Current address of W. Peng: Aker Kværner Offshore Partner AS. Postboks 8006, 4068 Stavanger, Norway.

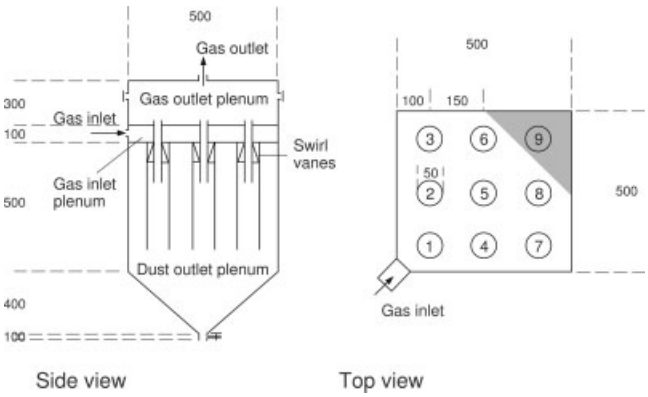

Figure 1. Swirl deck or multicyclone used for this work. Lengths are in mm. The grey area was blinded off by inserting an extra wall when the inlet was from the side.

gas from the hopper). This imbalance thus results in some "blow-down" of gas out of one or more of the cyclones and a compensating upflow of gas in one or more of the remaining cyclones. The blow-down does not negatively affect separation performance and actually improves the solids collection performance of those cyclones experiencing blow-down. However, the upflow destabilizes the vortex in the tubes, reducing the separation efficiency, or even leading to clogging. This may seriously impact the separation performance of swirl deck. The extent of the impact relates to both the extent of the inlet maldistribution and to the "tolerance" of the cyclones to upflow as established by the design.

Reznik and Matsnev[2] studied the characteristics of multicyclones, and state that the multicyclones usually have lower separation efficiency than an isolated cell under similar conditions. Crane and Behrouzi[3] list a number of reasons for such a discrepancy:

- Inlet flow maldistribution;
- Gas circulation in the common dust hopper leading to reentrainment;
- Loss of collected dust-loaded air through gaskets;
- Plugging of dust in gas exits or swirl vanes.

In fact, all the aforementioned phenomena are connected with cross-talk in the dust plenum. They found that installing baffle plates in the hopper can suppress the circulating flow and cross-talk, and, therefore, reduce dust emissions. They state that it is possible that the highly turbulent flows, which they observed in the multicyclone dust exit chamber, could be minimised by having opposite swirl direction in adjacent cells. They furthermore found that vortex stabilising cones had very little effect on the overall efficiency of the multicyclones.

Gauthier et al.[4] presented a method to eliminate the maldistribution by using a downward helical roof of the multicyclone, such that the inlet plenum becomes lower moving away from the gas inlet. However, a problem with the helical roof can be the varying lengths of the gas outlet ducts.[3,5] This difference in length creates a pressure drop difference between the back and the front tubes, causing gas circulation in the common dust hopper with gas flowing out of the front tubes, across the dust hopper, and up through the tubes in the back row.

Sage and Wright,[6] and Behrouzi and Crane[7] demonstrated the effectiveness of an underflow or "bleed" for both a single and a multicyclone configuration. Both configurations achieved emission reductions of some 30% with underflow rates of around 10%, as well as improved grade collection efficiencies for particles smaller than 5 μm.

In two recent articles,[8,9] the present authors have explored the flowpattern in single swirl tubes and cyclones with emphasis on the phenomenon known as the "end of the vortex" using a variety of experimental techniques, among other flow visualization using neutrally-boyant helium bubbles as tracer.

The objective of this work was to answer a number of questions around the important, but not very well understood, phenomenon of cross-talk and, more generally, the operation of centrifugal separators in parallel. Does lengthening the individual tubes improve the performance of the deck, or exacerbate cross-talk? Does cross-talk severely reduce performance of the deck compared with a single tube? Do atypical conditions in a single tube disturb the functioning of the deck as a whole severely? How does the vortex end phenomenon manifest itself in the deck, and is cross-talk recognizable in the flowpattern in the dust plenum?

Experimental Setup and Program

Experimental setup and conditions for the separation performance tests

Test Rig. The experiments were performed using a reduced scale (1:4) perspex model of an industrial swirl deck, which was shown in Figure 1. The rig layout is sketched in Figure 2. The absolute roughness of the perspex as delivered was about 6.4 μm.

A roots-blower is used to draw air loaded with dust using a sandblasting nozzle through the cyclone. The sandblasting nozzle is fed from a vibrating gutter and pneumatically transported to the nozzle. From the sandblasting nozzle, the dust is transported with the air into the cyclone system where most of the dust is captured. The captured dust is collected in the dust hopper, while the emitted dust is filtered out of the air by a large, membrane-coated filter bag, which can be weighed *in situ*. Under the bag a metal plate is built in, making it possible to collect the emitted dust for analysis.

Each experimental run with a given configuration lasted two hours, during which the volumetric gas flow and the dust load

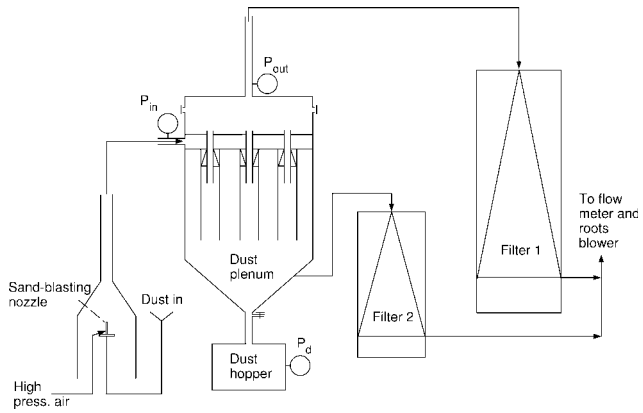

Figure 2. The system used.

were precisely controlled. The performance was assessed by determining:

- the percentage overall gravimetric separation efficiency (η),
- the pressure drop inlet, P_{in} to gas outlet P_{out} (ΔP)
- the pressure drop inlet P_{in} to dust outlet P_d
- the solids-mass balance over the equipment.

Measurements

There are a number of points in the system where the static gauge pressure can be measured. The pressure points relevant to the present work are indicated in Figure 2.

The gas flow through the system is measured with an "Annubar" flow meter, a metering principle similar to that of a pitot-tube. The manufacturer has provided an equation for calculating the volume-flow at normal condition (1 bar, 293K) through the annubar from the pressure difference measured. The manufacturer-supplied calibration of the Annubar was checked by the "Nederlands Meet Instituut" (NMI).

During an experiment the pressures were measured every 15 min for a period of approximately 2 h. A volume flow of 410 m^3/h, and a solids loading of 1.6 g/m^3 were used in all the experiments.

The pressure drops calculated from an experiment are the pressure drop inlet to outlet: $\Delta P = P_{out} - P_{in}$, and the pressure difference between the inlet and the dust outlet: $P_d - P_{in}$ (see Figure 2).

The pressure drops reported are averages of the pressure readings during the two-hour experiments. The high-time resolution sensors used to measure the pressure drops were of the type PTX 120/WL with accuracy of 0.1% from Druck Nederland bv.

Experimental procedure and calculations

The concept of equilibration of wall deposits was used during the experiments. Equilibration was achieved by prerunning the test rig under the same conditions as in the subsequent experiment, to make the walls of the inlet and outlet tubes "saturate" with dust. The idea is, thus, that the dust in the inlet and gas outlet plenums, and the inlet and outlet tubing, equilibrates, so that these parts need not be cleaned and the dust collected and weighed after every experiment.

The following solids masses were determined after each experiment:

- captured in the collection vessel m_h,
- captured in the filter m_{fb},
- captured in the underflow filter (filter 2) m_u,
- deposited in the conical dust plenum m_p, and
- deposited in and on the tubes and on the rectangular dust plenum section m_r,

Then the dust emitted equals

$$m_{em} = m_{fb} \tag{1}$$

The dust captured equals

$$m_{cap} = m_h + m_u + m_p + m_r \tag{2}$$

For the mass balance, the percentage loss of dust can be calculated from

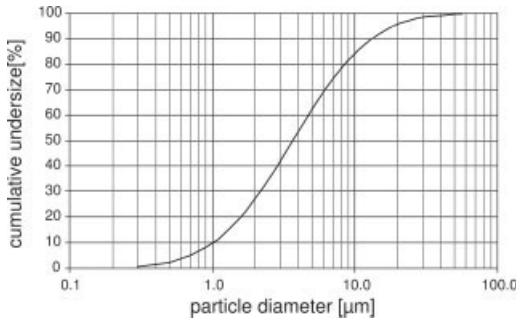

Figure 3. Size distribution of the test dust.

$$\text{percentage loss} = \frac{m_{cha} - (m_{fb} + m_h + m_u + m_p + m_r)}{m_{cha}} 100 \tag{3}$$

where m_{cha} is the mass charged. The overall percentage efficiency is equal to

$$\eta = \frac{m_{cap}}{m_{cap} + m_{em}} 100 \tag{4}$$

The average dust load was calculated from the average mass flow of dust and the average volumetric flow of air.

Experimental materials and conditions

The aim of the performance tests was to compare the performance with the performance of a single swirl tube to assess any detrimental effects of parallel operation, and to test some very specific geometrical configurations.

The test powder used is $CaCO_3$ with a particle density of 2,730 kg/m^3, which was mixed with 1% Snowcal SiO_2 in order to enhance the flow behavior. It had a size distribution (see Figure 3) such that the separation performance in the test rig with air under ambient conditions was comparable to that of the industrial cyclones under plant conditions. The size distribution was determined in a Joyce-Loebl disc centrifuge using a buffered line start technique.

Two swirl tube lengths were tested: 178 mm and 118 mm. Two inlet/outlet configurations were tested, the default, which was inlet at the side of the gas inlet plenum and outlet at the top, and an alternative where the two were switched (see later). Some repeat experiments were performed to check the reproducibility of the results.

Table 1 shows the experiments performed. The repeats of the first and the third experiments were used to calculate pooled estimates of the experimental error in the individual results, which came out to be 1.16% and 79.1 Pa for the efficiencies and the pressure drops, respectively. Table 1 reports the standard deviations of the *averaged* results.

For all the tests, the experimental conditions were:

- Dust load: 1,6 g dust/m^3 gas.
- Volumetric gas flow rate: 410 m^3/h, giving a mean velocity in the inlet tube to the plenum of 34 m/s.
- Gas underflow: 3%.

Table 1. Experimental Conditions and Errors

Geometry	(Q m^3/hr)	Std. dev. in $\langle\eta\rangle$ (%)	Std. dev. in $\langle P_{in} - P_{out}\rangle$ (Pa)	Number of tests
Tube length 178 mm	410	0.44	29.9	7
Tube length 118 mm	410	1.16	79.1	1
Tube length 178 mm (top in, side out)	410	0.67	48.6	3

Flow visualization test rig and procedure

The flow visualization tests were done by feeding helium bubbles with the same density as air. The deck model was the same as that used for the performance tests, but a perspex plate was used to replace the pyramid section underneath to be able to photograph the flow pattern in the dust plenum (Figure 4). This replacement probably does influence the flowpattern in the plenum somewhat, but the main interest was the flow close to, and between, the tube exits.

The swirl deck used for flow-visualization was a 8-tube configuration, tube No. 9 was closed for these experiments, as shown by the shaded area in Figure 1, in order to model the flow in the industrial unit more faithfully.

The helium bubble generator is Model 5 from Sage Action Inc. and produces helium-filled, neutrally buoyant bubbles as tracer for flow visualization, suitable for gas velocities up to about 70 m/s. The bubbles are made with a proprietary bubble film solution. Illumination is achieved with a 300 W Tungsten-Halogen Lamp, both from the supplier of the bubble generator.

The bubble generator was connected to the inlet tubing of the swirl deck, and a 70 mm thick light sheet was used to illuminate the plenum just under the tubes. A high-speed camera, on which the exposure time and frequency could be adjusted over wide ranges by software, was used to photograph the tracer bubbles moving in the plenum. Velocity information was gleaned from the images by (automatically) recognizing individual tracer bubbles on successive frames, determining the distance between them, and dividing by the time interval between frames. The velocity information was then finally averaged over time. The data preparation and analyses were executed by the commercial software packages Labview Vision and DiaTrack 2.3.

No powder was injected when performing helium-bubble flow visualization, but in separate visualization experiments powder was injected to observe striation patterns on the wall, an organic starch powder was used for this rather than the test dust described in the previous section. Starch normally has a particle size in excess of 10 μm, and is, therefore, easily separated in the cyclones, it was not used to assess separation efficiency.

Experimental Results

Efficiency and pressure drop

The equilibration procedure successfully resulted in a closed mass balance over the rig. The dust loss was less than 3% and the results were reproducible, as shown in Table 1.

The experimental results for the efficiency and the pressure drop gas inlet to gas outlet are shown in Figure 5.

In general one would expect the separation efficiency to increase as the pressure drop over the separator increases, and, therefore, an upward-going trend in the plot. The figure shows some spread in the seven results obtained with the long tubes, but the average efficiency is significantly higher than the efficiency with the short tube, even though the pressure drop using the long tubes is also significantly lower than the pressure drop using the short tubes.

Thus, lengthening the individual tubes had the effect of improving the overall performance of the deck. This is in line with earlier experimental results obtained in single cyclones and single swirl tubes,[10,11] which showed that even though the increased wall friction in a longer tube reduces the vortex intensity, therefore tending to reduce the efficiency, the longer separation space has a stronger beneficial effect on the efficiency.

The average efficiency and pressure drop for the long-tube, top-in, side-out geometry were: 93.8% and 5,337 Pa, respectively. The performance of this configuration was, therefore, the best of all due to the very low pressure drop. This low pressure drop, however, is not directly related to the swirl tube

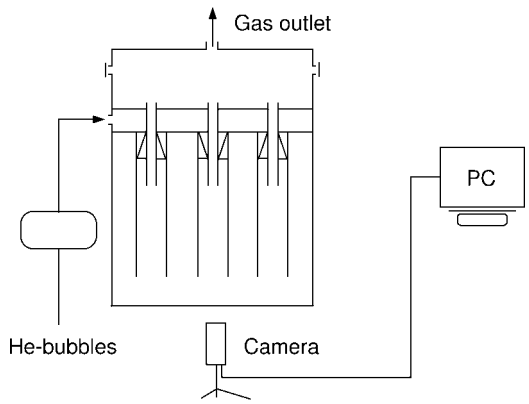

Figure 4. Flow pattern test rig.

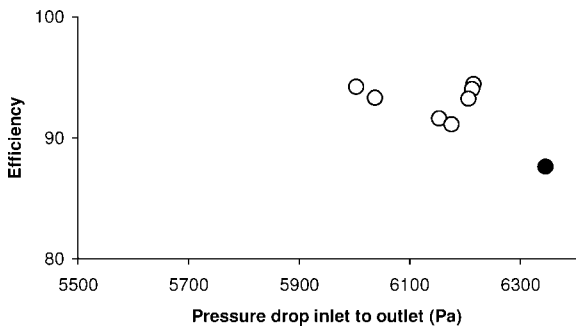

Figure 5. Effect of the tube body length on the performance. Open circles: long body, filled circles: short body.

arrangement in the deck, but rather to the geometries of the upstream and downstream plenums and ducting.

In order to compare with model predictions and with the performance of other separators through scaling, the experimental results have to be converted into a cyclone cut size. If we know the cumulative volumetric-size distribution of the feed

$$F(d_p) = \int_0^{d_p} f(x)dx \tag{5}$$

such that $F(d_p)$ is the volume fraction of powder with a particle diameter less than d_p, and we assume that all material below the cut size d_{p50} is lost and all above is collected by the cyclone, we can calculate d_{p50} from[1]

$$F(d_{p50}) = 1 - \eta \tag{6}$$

We note at this point that this is a serious simplification, especially in the present case where the particles captured are so fine. The grade-efficiency curves of the separators are likely to exhibit "duck-tailing", meaning that the separation efficiency actually rises with decreasing particle size for very fine particles. If this is the case, the earlier procedure will lead to unrealistically low-cut sizes.

For our feed powder, $F(d_p)$ is well approximated by a log-normal distribution with a mean $\langle \ln(x) \rangle$ of 1.3 and a spread σ of 1.0, that is,

$$f(x) = \frac{1}{x}\frac{1}{\sigma\sqrt{2\pi}} \cdot \exp\left(-\frac{(\ln x - \langle \ln x \rangle)^2}{2\sigma^2} \right) \tag{7}$$

where x the the particle diameter nondimensionalized with the scale length of $d_{p0} = 1$ μm, that is: $x = d_p/d_{p0}$, and σ is the standard deviation of the x.

The result of calculating the cut sizes in this way are: $d_1 = 0.54$ μm for the long body length and, $d_2 = 0.81$ μm for the short one.

We can compare the performance achieved in the swirl deck model with that achieved in a single, geometrically similar, but much larger, swirl tube. We do this by using the conventional scaling rules[1] that the Stokes number for the cut size, Stk_{50} and the Euler number, Eu should be the same in the two separators. Thus

$$(Stk)_{50,st} = \left(\frac{\Delta\rho d_p^2 v_{ch}}{18\mu D} \right)_{st} = \left(\frac{\Delta\rho d_p^2 v_{ch}}{18\mu D} \right)_{sd} = (Stk)_{50,sd} \tag{8}$$

and

$$(Eu)_{st} = \left(\frac{\Delta P}{\rho v_{ch}^2} \right)_{st} = \left(\frac{\Delta P}{\rho v_{ch}^2} \right)_{sd} = (Eu)_{sd}, \tag{9}$$

where subscript st refers to the single tube and sd to the swirl deck model. The characteristic velocity, v_{ch} is taken as the superficial-axial velocity in the tubes. Once the cut diameter has been found from Eq. 8, this can be converted to a percentage efficiency using Eq. 6.

The performance of the single swirl tube was calcuated as the average of a large number of experimental results, some of which are reported in.[11] The average overall efficiency with the same test dust as used in this work was 91.6%, corresponding to a cut size of 0.92 μm by Eq. 6.

Table 2. Predicted and Measured Performance of the Swirl Deck

Performance indicator (swirl deck)	Predicted from performance of single swirl tube	Experimental (averages)
η (%)	94.4	93.8
ΔP (Pa)	4160	5336

Table 2 compares the percentage efficiency actually achieved in the swirl deck with that predicted from the results in the single swirl tube using Eqs. 8 and 9.

It is clear that the separation efficiencies are consistent between the swirl deck and the single tube (bearing in mind the factors mentioned above about the shape of the grade-efficiency curve in the fine end). We can in any case conclude that the swirl tubes in parallel work close to the efficiency achieved by a single swirl tube. Thus this comparison shows that the performance of the swirl deck is not seriously reduced by effects, such as cross-talk.

The significant discrepancy in the predicted and measured pressure drops is as expected: in the single swirl tube there is still strong swirl present at the outlet pressure point, while there is none at the outlet pressure points in the swirl deck. Experience shows that this can cause the measured pressure drop in the single tube to be some 30% lower than in multiple tube units, which is also the difference we see in the table.

Effect of flow pattern in the gas-inlet plenum

Although a small insert was constructed at the inlet of the chamber to avoid an air jet effect into the chamber, the powder deposition patterns on the floor of the inlet chamber after experiments exhibit a clean area diagonally along the direction of the air jet in the chamber and powder buildup on the remainder of the plenum floor. To avoid this jet-effect, also a top-inlet, side-outlet configuration was tried. In this configuration the shaded tube in Figure 1 was opened, and the central tube just under the top inlet closed. In this case, the floor was clean in the center under the inlet, and the powder deposition was circularly symmetric around the inlet, with the powder deposits quite thick in the corners. The deposition patterns are sketched in Figure 6.

We can conclude that both inlet configurations create a flow in the inlet plenum. However, it turned out that both inlet configurations had the same high separation efficiency, indicating that these flows in the inlet plenum are not crucial in determining the performance.

Effect of the flow pattern in the tubes themselves

It is well known that rough walls will reduce the intensity of the vortex in a centrifugal separator, which in turn leads to a significantly *lower* pressure drop[1] and reduced separation efficiency. It is a question whether differences in the wall roughnesses of the individual tubes can lead to imbalance between the tubes.

The roughness of the wall in one of the tubes was increased by attaching sand-paper to the inside of the tube. It was not possible to see a significant change in either the separation efficiency or the pressure drop due to this modification.

Between the inlet and gas outlet plenums, the tubes play a similar role to simple tubes connected in parallel between two

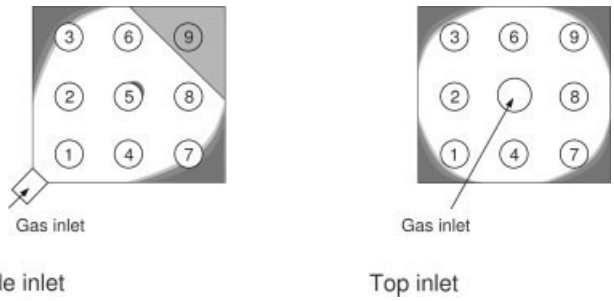

Figure 6. Sketch showing the powder deposition patterns with the two different-flow configurations used.

plenums. Changing the pressure drop over one (for example, by increasing its diameter) keeping the total flow constant will only result in a redistribution of the flow between the tubes, but no pressure imbalance, and no significant change in the pressure drop between the plenums.

The crucial thing in determining imbalance between tubes and cross-talk is what takes place in the bottom of the tubes, by the dust outlet plenum. In the following section we look more closely at this issue.

Visual Observations, Flow Visualization and Pressure Measurements

Visual observations

Observing the deck during operation with dust injection soon made it clear that the phenomenon known as the "end of the vortex"[8] was present in some of the tubes, evidenced by the formation of rings in those tubes.

In order to learn more about the phenomena, we ran a series of experiments using a gas flow rate of $Q = 388$ m^3/h without underflow, feeding powder with the gas.

Figure 7 shows a sequence of photos of this phenomenon, the insert in the first picture shows the region photographed.

The appearance of the vortex end in some of the tubes may well be related to cross-talk. The pressure in the bottom of tubes with and without the vortex end in the separation space is likely to be different, giving rise to flow through the plenum from one to the other. At the same time, upflow in a tube is known to cause the end of the vortex to move upward (destabilize the vortex further), such that it is likely that those tubes with the rings are "receptor" tubes.

Speaking against this is that other results have shown that in a single swirl tube or cyclone, a considerably *lower* pressure is measured in the dust hopper section if the vortex is centralized, so that the vortex end is not in the separation section of the tube. At this point we think that dissappearance of the ring in a tube in the deck means that the vortex just bends to the lip of the tube, so that the end of the vortex is at the bottom of the tube (see the following also).

Measurements using high-time-resolution pressure transducers

In order to study this phenomenon further, pressure tappings were constructed in the tubes.

High time-resolution pressure measurements were done at point 1 in tube No. 2 and point 4 in tube No. 3 (see Figure 8)

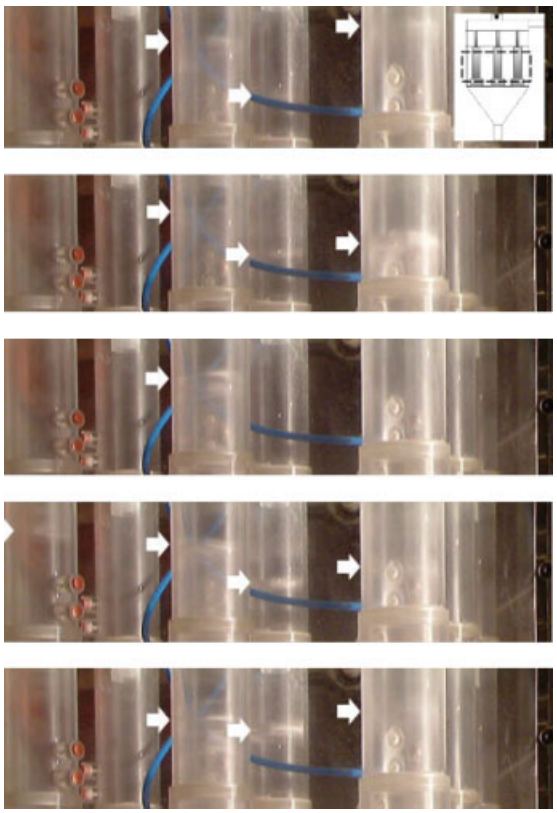

Figure 7. A series of photographs showing the ring formation in some of the tubes.

The rings can be seen to be changing position, and sometimes disappear completely from tubes. Test configuration: long tubes. [Color figure can be viewed in the online issue, which is available at www.interscience.wiley.com.]

with a gas flow rate of $Q = 388$ m^3/h, without underflow and without dust injection.

The results are shown in Figures 9 and 10. Consistent with earlier results in single separators, the pressure profile exhibits periodic pressure troughs, evidence of the vortex core passing over the pressure point as it rotates rapidly around the wall, creating, in the presence of dust, the appearance of a dust ring as seen in Figure 7.

The troughs are, although regular in time, somewhat irregular in depth, showing that the end of the vortex is moving axially somewhat randomly. Visually, this gives the impression that the rings are "dancing" in the tubes.

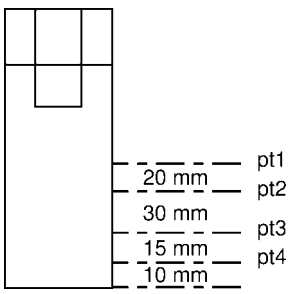

Figure 8. Sketch showing the positions of the pressure tapping installed in the swirl tubes.

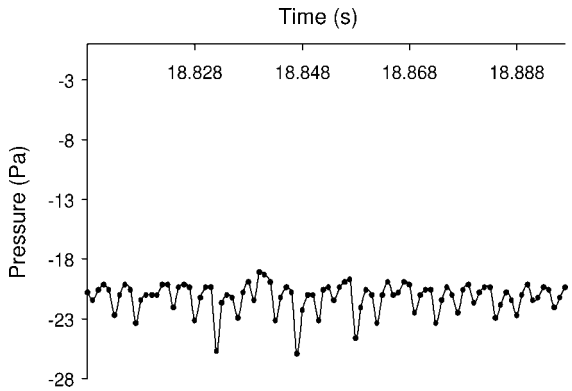

Figure 9. Pressure fluctuations at pressure tapping No. 1 in tube No. 2, showing the presence of the vortex end in the neighborhood of the pressure tapping.

Test configuration: long tubes.

Powder deposition pattern after a run

It has been shown before that a sudden increase in wall deposits exists at the lowest position of the end of the vortex after an experimental run.

Figure 11 shows the pattern after a run. Powder inside tubes 2 and 4 is evident, and this was the case irrespective of the length of the tubes used. These two tubes are probably the "receptor" tubes.

Flow Pattern in the Swirl Deck Dust Plenums

Visualization using high-speed camera

Figure 12 shows the result of the flow visualization procedure and analysis. A vortex motion is evident in the figure. This vortex motion was not stable in time, the vortex was moving.[1] Another feature seen in the figure is that gas is entering tube number 4, which is then a "receptor" tube, consistent with the other evidence presented earlier.

Visualization using the digital camera with controlled exposure time

Figure 13 shows the result of illuminating the dust plenum with a 20 mm thick light sheet, and photographing tracer bubbles with a digital camera with known exposure time. Also this technique reveals a vortex motion in the dust plenum similar to the one seen by the technique in the previous section.

Further discussion

The flowpattern in the dust plenum of cyclone decks has, in the past, widely been considered to be an important factor affecting cross-talk, and various modifications of the plenum geometry to obtain a more quiescent plenum have been discussed and tested.

In[8,9] it is shown not only that the vortex core may bend to the wall and precess around this at the point of the "end of the vortex", but also that, even if the end of the vortex is not visible in the tube, the core may well still be attached to the lip of the tube. The core does not easily (although it may do so) bridge

[1]The data shown in the figure are, as mentioned, the result of an averaging over a period of time. This time period is long relative to turbulent velocity fluctuations, but not long relative to changes in the mean flow.

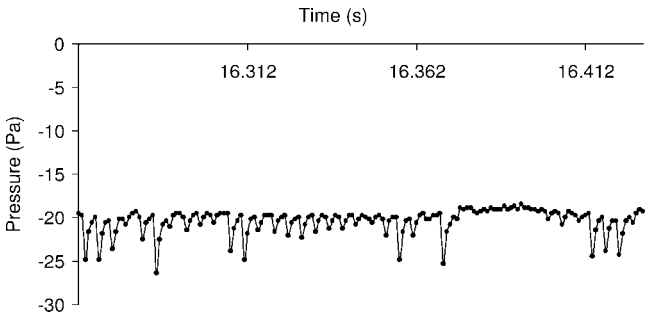

Figure 10. Pressure fluctuations at pressure tapping No. 4 in tube No. 3.

Test configuration: long tubes.

the large-diameter dust collection vessel to remain in the neighborhood of the swirl tube axis, and attach itself to the bottom of the dust collection vessel.

During these experiments, we did not see a strong swirling motion underneath the swirl tubes, and we did not see strong turbulence in the plenum. We, therefore, do not think that the vortex core extended to the floor of the dust collection plenum below any of the tubes, but rather was attached to the tube lip even in those tubes where we could not see the end of the vortex. Even so, we might expect that a vortex motion would exist in the dust plenum below and around each tube due to the formation of secondary vortices created by the vortex precession in the tube.[8]

Studying Figure 12, rotational motion around tubes 7 and 8, counterclock-wise and clockwise, respectively, is evident. A weaker counterclockwise rotation is seen around tube 5, while the picture is not entirely clear around tube 4. Keeping in mind that the filming is from the bottom the senses of rotation are consistent with the senses of rotation in the tubes themselves; the tubes were equipped with vanes causing rotation with alternate senses.

Donor tubes are likely to disturb the plenum flow around them more than receptor tubes, consistent with the observation that the rotation around tube 4, which, as mentioned, appears to be a receptor tube, is only weak.

With the vane arrangement as described, the rotation around two neighboring tubes will not give rise to the formation of a secondary vortex between them. Two diagonally neighboring

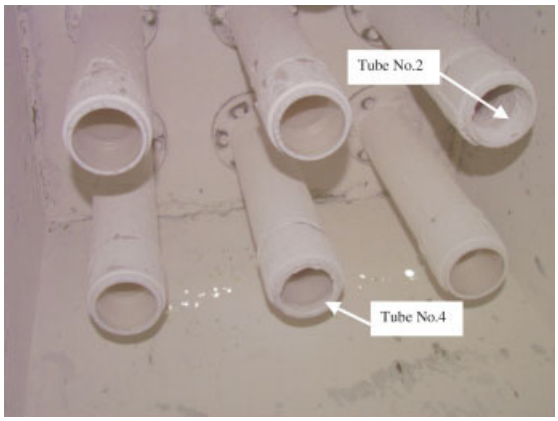

Figure 11. Powder deposition pattern after a test.

Test configuration: long tubes. [Color figure can be viewed in the online issue, which is available at www.interscience.wiley.com.]

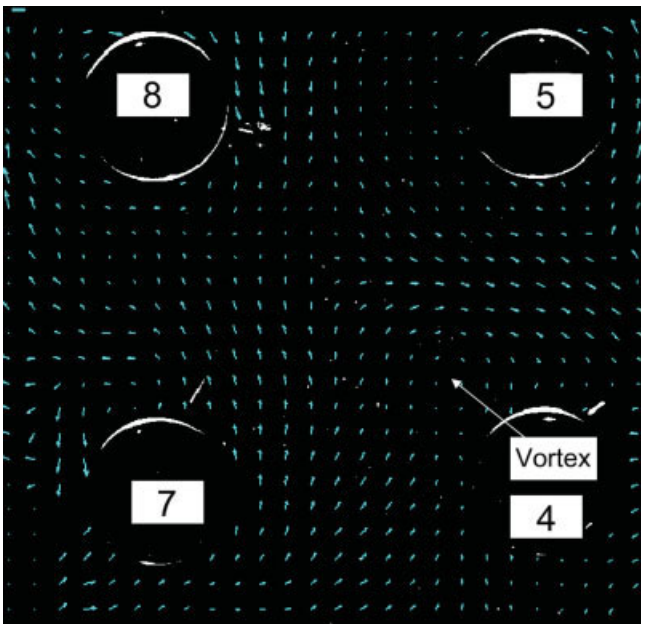

Figure 12. Mean velocity pattern in the dust plenum by flow visualization.

Test configuration: long tubes. [Color figure can be viewed in the online issue, which is available at www.interscience.wiley.com.]

tubes, however, turning in the same sense, might. Tube pairs 8 and 4 and 7 and 5, respectively, will, however, tend to create secondary vortices of the opposite sense. If the rotation around one of the tube pairs dominates (tubes 7 and 5 in this case, seeing the sense of the vortex motion between the tubes) a secondary vortex might be formed, and this may explain the vortex motion marked in the figure.

At this point we make some remarks about the relation between the method used here for quantifying the plenum flow field and the method of particle image velocimetry (PIV). In a laboratory sized system the number density of the helium bubbles is so low that tracking each bubble separately is necessary, meaning that a large number of frames must be analyzed to obtain a mean velocity field, and that a complete picture of the instantaneous flow field cannot be gleaned. This is in contrast to PIV, where a laser light sheet illuminates a large number of fine tracer particles, and the instantaneous velocity field is obtained by cross-correlating subsequent exposures of the same cells of a spatial grid. The resolution in PIV depends on the size of the cells of this grid. A mean flow field can be obtained from PIV by averaging over time. This may be done in more than one direction using two cameras for stereoscopic PIV.

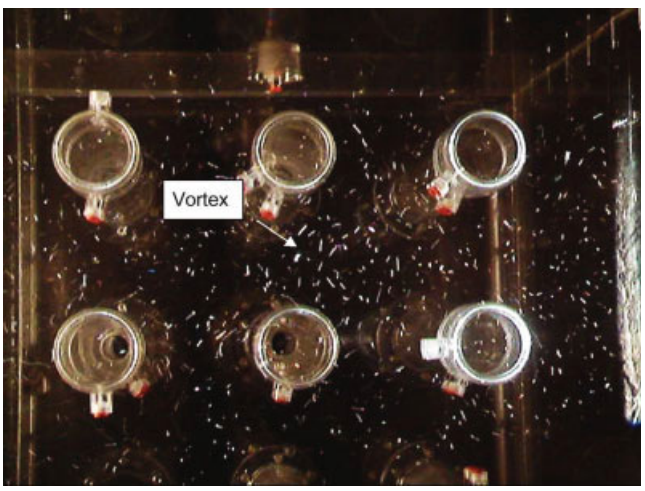

Figure 13. Flow visualization in the dust plenum with controlled-exposure photography of the tracer bubbles.

Test configuration: long tubes [Color figure can be viewed in the online issue, which is available at www.interscience.wiley.com.]

A problem, however, with PIV and other techniques is the faithfulness with which the tracer particles—which are fine but normally have a density much higher than that of air—follow the gas stream. The helium bubbles used in this study, having the same density as air, will, as discussed in[9] faithfully follow the gas stream even in strongly swirling or turbulent flow. The only limitation in this respect is the size of the bubbles, which is of the order of 1 mm, and, therefore, larger than the very finest turbulent eddies, the size of which is given by the Kolmogorov length scale. As shown in,[9] however, the eddies smaller than the bubbles will in most systems relevant to process technology be well within the dissipative range of the turbulence, and, therefore, not a very significant feature of the flow field.

It is conceivable that helium bubbles could be used as tracer in a PIV analysis if the system is large enough relative to the bubble dimensions.

Conclusions

- The efficiency of the deck was only marginally lower than that predicted on basis of results in a single, but larger, swirl tube. The performance of the deck improved when prolonging the tubes.
- The system of swirl tubes working in parallel was found to be somewhat "forgiving" when applying disturbances, such as different gas inlet configurations and artificial wall roughness in one of the tubes.
- Evidence of the vortex end was seen in some of the tubes, both by ring formation when running with dust injection and with high-time-resolution pressure sensors. The behavior of the vortex end was erratic and unsteady.
- The tubes with the vortex end in them are likely to be "receptor" tubes in a cross-talk situation, this was confirmed by the flow-visualizations in the dust plenum
- Flow-visualizations in the dust plenum were able to pick up vortex motion in the plenum, both around the individual tubes and sometimes between the tubes.

Acknowledgments

We gratefully acknowledge the dedicated and expert support we continually receive from the workshop at the Dept. of Physics and Technology, University of Bergen.

Notation

d_p = particle size (diameter)
d_{p50} = separator cut size
D = diameter of the swirl tube
Eu = Euler number
Eu_{sd} = Euler number in a tube in the deck
Eu_{st} = Euler number in a single tube
$f(\cdot)$ = differential-size distribution
$F(\cdot)$ = cumulative-size distribution
m_{cha} = powder-mass charged

m_{cap}, m_{em} = total masses captured and emitted
m_{fb}, m_h, m_u = mass captured in main filter, hopper and underflow filter
m_p = mass deposited in conical dust plenum section
m_r = mass deposited in tubes and rectangular dust plenum section
P = pressure
P_d = pressure in dust collection vessel
P_{in} = inlet pressure
P_{out} = gas outlet pressure
Q = volumetric gas flow rate
Stk = Stokes number
Stk_{50} = Stokes number for the cut size
Stk_{sd} = Stokes number in a tube in the deck
Stk_{st} = Stokes number in a single tube
x = dimensionless particle size
v_{ch} = characteristic velocity

Greek letters

Δ = difference in
η = overall gravimetric efficiency
μ = viscosity
ρ = density
σ = standard deviation

Literature Cited

1. Hoffmann AC, Stein LE. *Gas cyclones and swirl tubes—Principles, design and operation*. Heidelberg: Springer Verlag; 2002.
2. Reznik VA, Matsnev VV. Comparing characteristics of elements in batteries of cyclones. *Thermal Eng* 1971;18:34–49.
3. Crane RI, Behrouzi P. Evaluation and improvement of multicell cyclone dust separation performance. *Industrie Minérale-Mines et carrières—Les techniques*. 1991;73:154–161.
4. Gauthier TA, Briens CL, Bergougnon MA, Galtier P. Uniflow cyclone efficiency study. *Powder Technol*. 1990;62:217–225.
5. Crellin B, Bennellick KRJ, Marshall AB. Improved particulate emission control for solid fuel fired boilers *Appita*. 1980;33:345–350.
6. Sage PW, Wright MA. The use of gas bleeds to enhance cyclone performance. *Filtration and Separation*. 1985;Jan/Feb:32–36.
7. Behrouzi P, Crane RI. Multicell cyclone separator performance with secondary gas extraction. *Gas-Solid Flows*. 1991;121:273–278.
8. Peng W, Hoffmann AC, Dries HWA, Regelink MA, Stein LE. Experimental study of the vortex end in centrifugal separators: The nature of the vortex end. *Chem. Eng. Sci*. 2005;60:6919–6928.
9. Peng W, Hoffmann AC, Dries HWA, Regelink MA, Foo K-K. Neutrally buoyant tracer in gas cleaning equaipment: a case study. *Meas Sci. and Technol*. 2005;16:2405–2414.
10. Hoffmann AC, Groot M, Peng W, Dries HWA, Kater J. Advantages and Risks in Increasing Cyclone Separator Length. *AIChE J*. 2001;47:2452–2460.
11. Peng W, Hoffmann AC, Dries H. Separation characteristics of swirl tube dust separator *AIChE J*. 2004;50:87–96.

Manuscript received Jun. 2, 2006, revision received Nov. 6, 2006., and final revision received Dec. 28, 2006.